On three-body Coulomb dynamics in hydrogen ionization by protons and antiprotons at intermediate collision velocities

A.B.Voitkiv and J.Ullrich

Max-Planck-Institut für Kernphysik,

Saupfercheckweg 1, D-69117 Heidelberg, Germany

(Dated: April 14, 2003)

Abstract

We consider ionization of atomic hydrogen with emission of low-energy electrons by proton and antiproton impact in the range of impact velocities 3 a.u. $\leq v_p \leq$ 6 a.u., where the electron capture by protons is already of minor importance but the differences in hydrogen ionization due to proton and antiproton impact can still be substantial. By calculating various differential cross sections within the first and second Born and CDW-EIS approximations we attempt to analyze the dynamics of hydrogen ionization by protons and antiprotons. We discuss in some detail the role of : i) the interaction between the projectile and the target nucleus and ii) multiphoton exchanges between the projectile and the target electron. Profound charge-sign effects are suggested by CDW-EIS and second Born calculations for the fully differential emission pattern. Although after the integration over the electron emission angles these effects substantially diminish, they still remain noticeable even in the total ionization cross section suggesting, in particular, that protons are more effective, compared to antiprotons, in producing soft electron emission from hydrogen in the range of collision velocities under consideration.

PACS numbers: 34.10.+x, 34.50.-s, 34.50.Fa

Introduction

Scattering of a point-like charged projectile on atomic hydrogen represent the simplest and most fundamental case of the Coulomb three-body collision problem in quantum mechanics. One of the interesting phenomena which can occur in such collisions is hydrogen ionization in which all the three particles are finally unbound and constitute the three-body Coulomb continuum.

Since protons and antiprotons have the same mass, the comparative study of hydrogen ionization in collisions with these particles is important for understanding effects arising due to different signs of the projectile charges. According to the first Born approximation cross sections for hydrogen ionization should be proportional to Z_p^2, where Z_p is the projectile charge. Therefore, any considerable differences between hydrogen ionization by equivelocity protons and antiprotons would clearly display the break-down of this approximation.

There is a number of theoretical papers on hydrogen ionization by antiprotons in the low and intermediate collision velocity regimes (see [1]-[5]). In addition, few experimental results on hydrogen ionization by antiprotons are available for impact energies ranging from 30 keV to 1 MeV [6]. However, all the above mentioned papers were devoted to the study of the total ionization cross section as a function of the impact energy. To our knowledge, there is only one very recent paper [7] where the fully differential cross section for hydrogen ionization in the collision plane was considered in the context of the scaling properties of ionization by protons, antiprotons, electrons and positrons.

The study of differential cross sections in general can provide much deeper insight into the collision dynamics, compared to considerations of total cross sections only, representing a significantly stricter test for any theory. This is especially the case if the fully differential cross section (FDCS) is investigated. In this cross section initial and final states of all particles are fixed and, therefore, its exploration unveils the collision dynamics on the very basic level. Other differential cross sections which are very sensitive to the collision dynamics are those differential in both the electron and projectile variables.

Indeed, recent experimental and theoretical studies on helium single ionization by 100 MeV/u C^{6+} [8] and by 3.6 MeV/u Au^{24+} and Au^{53+} [9]-[11] have revealed that there is a striking disagreement between theory and experiment for the fully differential cross sections and for cross sections differential in the momentum transfer and electron emission energy.

Even for collisions with 100 MeV/u C^{6+} where the effective perturbation strength $Z_p/v_p = 0.1$ is quite small (v_p is the collision velocity) theory could not reproduce all essential details of experimentally measured cross sections [8]. Such disagreements between experiment and theory were not expected since it was known for quite some time that for helium single ionization the total cross section and cross sections differential only in the variables of the emitted electron (electron emission spectra) are well reproduced by theory.

The success of theory in describing ion-atom collisions is directly connected with two main points: i) the projectile-target interaction should be properly treated and ii) free target states should be known with good accuracy. When considering collisions with helium it is not clear to which of the points, i) or/and ii), the above mentioned failure of theory is to be attributed. In particular, results of quantum calculations turned out to be very sensitive to a choice of the effective three-body model to simulate the helium target in singly ionizing collisions (compare e.g. results of [9] and [11]).

The atomic hydrogen target, with its well known states, represents an ideal case for studying effects arising from the projectile-target interaction. Keeping also in mind that it may soon become possible to perform kinematically complete experiments for ionization of an atomic hydrogen by ion impacts, in the present paper we want to explore in some detail the collision dynamics for hydrogen ionization by equivelocity protons and antiprotons in the interval of collision velocities 3 a.u. $\leq v_p \leq$ 6 a.u.. We refer to such collisions, somewhat arbitrarily, as being in the regime of the intermediate collision velocities. We shall restrict our attention to the consideration of hydrogen ionization accompanied by emission of low-energy electrons the velocities of which with respect to the target nucleus do not noticeably exceed 1 a.u.. Such electrons are called soft electrons and they contribute most to the total emission from hydrogen.

The above interval of collision velocities has been chosen because of three main reasons. First, these velocities are high enough in order to ensure that the capture channel (in collisions with protons) is of minor importance for the total electron loss from hydrogen. Second, such collisions, on the other hand, are slow enough in order to still expect substantial differences between hydrogen ionization by protons and antiprotons. Third, our study shall be mainly based on the Continuum-Distorted-Wave-Eikonal-Initial-State approximation which is supposed to yield quite reasonable results for soft electron emission in the range of collision velocities in question (see the discussion on the applicability of this approximation in

the next section).

Atomic units are used throughout except where otherwise stated.

General

In order to treat hydrogen ionization by protons and antiprotons we will use, as a basic method, the Continuum Distorted Wave-Eikonal Initial State (CDW-EIS) approximation. We shall regularly compare results of the CDW-EIS with those given by the first Born approach. In addition, the second Born approximation will be used for considering the fully differential cross section.

The application of the first and second Born approximations for exploring atomic collisions has a long history. These approximations have been studied in great detail in the literature (see e.g. [12] and references therein) and will not be discussed here.

The CDW-EIS approximation was introduced in [13] by replacing the CDW description of the initial state by its asymptotic (eikonal) form. This approximation belongs to the family of perturbative distorted-wave theories and is rather well documented in the literature (see [13]-[17] and references therein, and also [18]). Most often the CDW-EIS approach is used in its semiclassical form, in which the projectile interaction with the target nucleus can be factored out and does not influence the electron transition probability. For heavy ion-atom collisions this form has been very successful in describing total ionization cross sections and electron emission spectra. In particular, the semiclassical form of CDW-EIS was applied to calculate the total cross section for hydrogen ionization by antiprotons giving excellent agreement with experimental data and results of other calculations for collision velocities $v_p \gtrsim 1.5 - 2$ a.u..

The "full" quantum version of this approach, where the projectile-target nucleus interaction is included, has yielded very good results for cross sections of helium ionization by protons differential in the projectile scattering angle [15]. Recently, it was applied to consider fully differential cross sections in the collision plane for soft electron emission from hydrogen due to electron impact with impact energies as low as $27.2 - 250$ eV (corresponding to the initial projectile-electron velocity of $1.4 - 4.3$ a.u.) and a good agreement with available experimental data and results of the nonperturbative Convergent Close Coupling approach was found [16]-[17].

In the present paper we apply the "full" quantum version of the CDW-EIS approximation for exploring soft electron emission from hydrogen by protons and antiprotons at collision velocities $v_p \geq 3$ a.u.. According to the above discussion, this method is expected to provide sound grounds for studying hydrogen ionization at these collision velocities.

The most detailed information about the ionization process can be obtained by considering the fully differential cross sections. In the case under consideration a fast heavy projectile can suffer only very small deflection in the collision and the velocity of the recoil ion (in a frame where the target is initially at rest) is negligible compared to that of the emitted electron. The fully differential cross section can be written as

$$\frac{d^5\sigma}{d^2\mathbf{Q}d^3\mathbf{k}} = \frac{1}{4\pi^2 v_p}|T(\mathbf{q},\mathbf{k})|^2 \tag{1}$$

Here $T(\mathbf{q},\mathbf{k})$ is the corresponding transition matrix element, $\mathbf{k}$ is the electron momentum in the final state with respect to the target nucleus and $\mathbf{Q}$ is the two-component transverse part of the total momentum $\mathbf{q} = (\mathbf{Q}, q_{min})$ transferred to the target in the collision. One has $\mathbf{Q}\cdot\mathbf{v}_i = 0$, where $\mathbf{v}_i$ is the initial relative projectile-target velocity. In hydrogen ionization by relatively fast heavy projectiles, where the initial and final projectile momenta are nearly identical ($\mathbf{v}_f = \mathbf{v}_i = \mathbf{v}_p$), the longitudinal component of the momentum transfer $q_{min} = \frac{\mathbf{q}\cdot\mathbf{v}_p}{v_p} = (k^2+1)/(2v_p)$ is fixed by the energy conservation in the collision.

In addition to the FDCS (1), we will consider another two cross sections differential in the transverse momentum transfer. The first one is differential in the absolute value of the transverse momentum transfer Q and the electron emission energy $E_k = k^2/2$

$$\frac{d^2\sigma}{dQdE_k} = 2\pi k \int d\Omega_k \frac{d^5\sigma}{d^2\mathbf{Q}d^3\mathbf{k}}, \tag{2}$$

which is obtained from the fully differential cross section (1) by integrating over the electron solid emission angle $d\Omega_k = \sin\vartheta_k d\vartheta_k d\varphi_k$, where $\vartheta_k = \arccos(\mathbf{k}\cdot\mathbf{v}_p/kv_p)$ and φ_k are the polar and azimuthal electron emission angles, respectively [20]. The second cross section is differential only in the transverse momentum transfer

$$\frac{d\sigma}{dQ} = \int_0^{E_{max}} dE_k \frac{d^2\sigma}{dQdE_k}, \tag{3}$$

where the integration over the energy of the emitted electron runs from 0 to some value E_{max}.

Further, we shall also consider cross sections for hydrogen ionization integrated over the momentum transfer $\mathbf{Q}$. Namely, we will calculate energy, longitudinal and transverse momentum distributions of electrons emitted from hydrogen by proton and antiproton impact. These distributions can be obtained by integrating (1) according to

$$\frac{d\sigma}{dE_k} = 2\pi k \int dQQ \int d\Omega_k \frac{d^5\sigma}{d^2\mathbf{Q}d^3\mathbf{k}}, \tag{4}$$

$$\frac{d\sigma}{dk_{\|}} = 2\pi \int dQQ \int d^2\mathbf{k}_{\perp} \frac{d^5\sigma}{d^2\mathbf{Q}d^3\mathbf{k}} \tag{5}$$

and

$$\frac{d\sigma}{dk_{\perp}} = 2\pi k_{\perp} \int d^2\mathbf{Q} \int dk_{\|} \frac{d^5\sigma}{d^2\mathbf{Q}d^3\mathbf{k}}. \tag{6}$$

In Eqs.(5)-(6) $k_{\|}$ is the longitudinal component of the total electron momentum $\mathbf{k}$, $k_{\|} = \mathbf{k} \cdot \mathbf{v}_p/v_p$, and $\mathbf{k}_{\perp}$ is the transverse (two-dimensional) part of $\mathbf{k}$, $\mathbf{k}_{\perp} \cdot \mathbf{v}_p = 0$.

Results and discussion

In this section we present results for three different values of the collision velocity: $v_p = 3$, 4.5 and 6 a.u.. This corresponds to proton/antiproton energies in the target frame varying roughly from 200 keV to 1 MeV. It is assumed that initially the hydrogen target is in the ground state and rests in the laboratory frame. All cross sections will be given in the laboratory frame. In collisions with protons a hydrogen target can loose an electron both due to the ionization and capture processes. The latter reaction is not possible in collisions with antiprotons. However, for collision velocities under consideration the total capture cross section in collisions with protons is already orders of magnitude smaller than the total ionization cross section and, therefore, will not be considered below.

Fully differential cross section in the collision plane

The collision plane is defined by the vectors $\mathbf{v}_p$ and $\mathbf{q}$ (in this plane one has $\varphi_k = 0^0$, see figure 1) and respective differential cross sections give important contribution to the total emission. In figures 2-4 we display results for the fully differential cross section (1) in the collision plane for proton and antiproton impact at velocities $v_p = 3$, 4.5 and 6 a.u.,

respectively. The results were obtained by using the CDW-EIS method and the first order Born approximation. It is seen that collisions with protons and antiprotons in general yield rather different emission patterns in the collision plane. Compared to first Born results the more sophisticated CDW-EIS theory predicts that the binary peak is enhanced (weakened) in collisions with protons (antiprotons), the contrary holds true for the recoil peak. In addition, CDW-EIS calculations suggest that both peaks are shifted compared to their positions predicted by the first Born approximation. The character of this shift depends on the sign of the projectile charge: for protons the binary peak is shifted to smaller angles and the recoil peak to larger angles, for antiprotons we observe the opposite tendency.

There are two main differences between the CDW-EIS and first order Born approximations which are responsible for the differences in predictions of these theories. First, the CDW-EIS not only accounts for the so called single photon exchange between the projectile and the target electron but also includes contributions from multiphoton exchanges between these particles. Second, within the first Born approximation the interaction between the projectile and the target nucleus (in the following also denoted as the $p-n$ interaction) has no impact on collisions which are inelastic for the target [21]. In contrast, according to the CDW-EIS the $p-n$ interaction may represent one of the important mechanisms of momentum exchange in the reaction having strong impact on the projectile scattering and, thus, on the fully resolved electron emission pattern.

In order to get some insight about i) the role of the $p-n$ interaction and ii) the relative importance of the multiphoton exchanges between the projectile and the target electron and the $p-n$ interaction, we have performed calculations where the latter was neglected. The results are also shown in figures 2-4. They suggest that the points i)-ii) can be very different for collisions with protons and antiprotons.

Let us first consider the binary peak. For collisions with protons one observes that if the $p-n$ interaction is switched off in CDW-EIS calculations then the result in the collision plane becomes considerably closer to that predicted by the first Born theory and very substantially differs from the result of that version of the CDW-EIS theory where all the interactions are taken into account. For antiproton impact the situation for emission in the collision plane is more complicated. In contrast to the case with protons, now the $p-n$ interaction seems to have an important effect on the shape of the emission pattern only provided the transverse momentum transfer Q reaches considerable values. Indeed, for the emission in the collision

plane by antiprotons we observe that, as far as the condition $k \gg Q$ holds, the role of the $p-n$ interaction remains rather modest: if this interaction is switched off, differences with first Born predictions are still very substantial and the results are close to those following from the CDW-EIS calculation including the $p-n$ interaction. However, if the condition $k \lesssim Q$ is fulfilled, then the situation with the points i)-ii) becomes similar to that in collisions with protons (see figure 4a,c). In such a case the interaction between the antiproton and the hydrogen nucleus is much more important and is responsible for the major part of the deviations from the first Born predictions for the collision plane.

For the recoil peak, which reaches considerable values only for relatively small momentum transfers, we observe that the correspondence between the $p-n$ interaction and the multiple photon exchanges in the projectile-electron interaction is contrary to that observed for the binary peak. In particular, now the $p-n$ interaction is always very important for collisions with antiprotons whereas switching off this interaction for collisions with protons does not drastically change the calculated shape of the recoil peak.

In addition to the first Born and CDW-EIS approaches we have also applied the second Born approximation for evaluating the fully differential cross section. In the latter approximation the closure approximation was employed in order to perform the summation over all intermediate target states. The closure approximation contains a free parameter - the mean excitation energy of the target. In accordance with known prescriptions (see e.g. [12] and references therein) this energy was chosen as 0.5 a.u.. Within the scope of the second Born approximation the projectile-target interaction is effectively reduced to just single- and double-photon exchanges between the colliding partners. Since the CDW-EIS approach is expected to be superior to the second Born one, the differences between results of these two approaches can serve as some indication of the importance of the third and higher-order terms in the corresponding perturbative Born series for the transition amplitude.

In figures 5 and 6 we present second Born results for collisions at $v_p = 4.5$ ($Q = 0.2$ and $E_k = 10$ eV) and at $v_p = 6$ (for $Q = 0.1$ and $Q = 1$ a.u., $E_k = 10$ eV). In these figures first Born and CDW-EIS predictions are also shown. In line with expectations it was found that the difference between CDW-EIS and second Born results on average decreases with increasing collision velocity. For example, one observes a rather good agreement between these calculations for $v_p = 6$ a.u. whereas at $v_p = 4.5$ they still differ considerably. At the same time at $v_p = 6$ the differences are, on average, more pronounced for collisions

with larger momentum transfers Q. A rather straightforward explanation of this correlation between the CDW-EIS and second Born results could be that both by increasing the collision velocity and by decreasing the momentum transfer Q we effectively weaken the projectile-target interaction and, therefore, reduce the contribution of the higher-order terms in the Born series.

Cross section $d^2\sigma/dQdE_k$

According to CDW-EIS calculations, the integration over the electron emission angles substantially reduces the difference between corresponding ionization cross sections for proton and antiproton impact, respectively. It is clearly seen in figures 7, where results for the cross section $d^2\sigma/dQdE_k$ are shown as a function of Q for $0.1 \leq Q \leq 3.5$, that this difference becomes much weaker compared to that observed in the fully differential cross section. One of the reasons is that, compared to first Born predictions in the collision plane, the binary peak was found to be enhanced in collisions with protons and the recoil one in those with antiprotons and after the integration over ϑ_k the difference decreases. The second reason is that for the emission out of the collision plane the CDW-EIS theory suggests different relations between proton and antiproton impact, compared to those discussed in the previous subsection.

Some other points concerning the shape of the cross section $d^2\sigma/dQdE_k$ seem to be worth mentioning.

First, figures 7a-c indicate and more extensive calculations show that the difference between the cross sections $d^2\sigma/dQdE$ for hydrogen ionization by proton and antiproton impact is negligible provided the electron emission energy is small enough, $E_k \lesssim Q^2/2$. Further, if, in such a case, the $p-n$ interaction is ignored in the CDW-EIS calculations, the latter yield results for the cross section which are quite close to those following from the first Born approximation. Thus, for electron emission in collisions with relatively large momentum transfers, $Q^2 \gtrsim E_k$, the effects of the second and higher orders in the interaction between the projectiles and the electron, *after the integration over the electron emission angles*, turn out to be much less important than the effect of the $p-n$ interaction (see figures 7a-c).

If one considers the cross section $d^2\sigma/dE_kdQ$ for a fixed value of the emission energy E_k, then for the "intermediate" values of Q (see figures 7a-c) the $p-n$ interaction decreases

the cross section [22]. In contrast, at "small" and "large" Q the inclusion of this interaction increases the cross section compared to first Born results.

At "large" Q the $p-n$ interaction makes it easier to fulfil the energy-momentum balance in the proton/antiproton-hydrogen ionizing collision. The latter is especially obvious for collisions at $v_p = 3$ a.u. (figure 7a). At this velocity, if the electron were free and at rest, the maximally possible proton/antiproton deflection angle in the proton/antiproton scattering on such an electron, $\vartheta_{max} = m_e/M_p$, would correspond to $Q = 3$ a.u. (m_e and M_p are the electron and proton/antiproton masses, respectively). Therefore, for momentum transfers close to 3 a.u. or larger any "assistance" by the direct projectile-target-nucleus coupling becomes essential [23].

Second, when, at a fixed v_p, the electron emission energy increases, the difference between the cross section due to proton and antiproton impact rises with the proton cross section being noticeably larger. We shall see in the following that the latter reflects the fact that, according to the CDW-EIS theory, in the range of collision velocities under consideration protons are in general more effective in producing soft electron emission as compared to antiprotons, especially for the higher-energy part of this emission. Such a larger "productivity" by protons remains in CDW-EIS calculations if one switches off the $p-n$ interaction.

Third, with increasing emission energy we observe that the cross section $d^2\sigma/dQdE$, as a function of Q, shows a strong non-monotonic behaviour with a maximum in the cross section roughly situated at $Q \sim k$. This reflects the importance of the "binary-encounter" collisions where the change in the projectile momentum is mainly balanced by the change in the electron momentum. Yet, even in these "binary-encounter" collisions the $p-n$ interaction may still play an important role resulting in the decrease and shift of the "binary-encounter" maximum in the cross section as compared to first Born predictions.

Cross section $d\sigma/dQ$

Shown in figure 8 are results of CDW-EIS and first Born calculations for the cross section $d\sigma/dQ$ at a collision velocity of 3 a.u.. The momentum transfer Q varies in the range $0.1 \leq Q \leq 2.5$. Here, we have integrated over all electrons with emission energies $E_k \leq 1$ a.u.. The CDW-EIS calculations were performed with and without including the $p-n$ interaction. It follows from the calculations that one can distinguish three ranges of the

momentum transfer Q, where one observes different correlation between first order and CDW-EIS results.

First, in the range of the relatively small Q ($0.1 \leq Q \lesssim 0.5$) the differences between results of the full CDW-EIS and first Born calculations are smaller than those between CDW-EIS results obtained with and without including the $p-n$ interaction. Thus, in this range the first Born approximation yields good results not because the contributions from non-first-order terms are themselves small but because there is a substantial cancellation in the cross section $d\sigma/dQ$ between the effect of the $p-n$ interaction and the effects of the multiphoton exchanges between the projectile and the electron.

In the range of the intermediate momentum transfers, 0.5 a.u. $\lesssim Q \lesssim$ 2 a.u., the effect of the $p-n$ interaction remains important and leads to the decrease of the cross section values compared to the first Born results. The higher-order contributions from the projectile-electron interaction, however, become of minor importance and continue to diminish with increasing Q.

With the further increase of Q ($Q >$ 2 a.u.) the effect of the $p-n$ interaction is to increase the cross section compared to the first Born prediction since, as we noted already, the $p-n$ interaction makes it easier to fulfil the energy-momentum balance in collisions with large Q. In the latter range of Q the effect of the multiphoton exchanges between the projectile and electron on the cross section $d\sigma/dQ$ is negligible.

In all the three ranges of Q the CDW-EIS calculations predict that the cross section is larger in collisions with protons. This is consistent with results of CTMC studies of the total cross section for hydrogen ionization by protons and antiprotons [1], although we found that the difference between the total cross sections is somewhat smaller than that predicted by CTMC.

For collisions at $v_p = 4.5$ and 6 the cross section $d\sigma/dQ$ behaves in the range $0.1 \leq Q \leq 2.5$ similarly to that at $v_p = 3$. For these larger v_p the above discussed peculiarities become less pronounced.

Electron distributions

If within the CDW-EIS method one performs the integration over the momentum transfer **Q** then the corresponding cross sections turn out to be practically independent of whether the

$p-n$ interaction is included or not. This is not very surprising because i) heavy projectiles like protons or antiprotons suffer only extremely small deflections at collision velocities under consideration and ii) the recoil ion, getting a negligible recoil velocity (estimated as $v_R \sim \max\{q,k\}/M_p \sim 10^{-3}$ a.u.), remains practically at rest. In such collisions ionization cross sections differential only in the electronic variables (energy, momentum, etc) are very well reproduced by semiclassical theories in which the projectile and the target nucleus are regarded as classical particles, the projectile is assumed to move along a straight-line trajectory and the target nucleus to be at rest and where the $p-n$ interaction can be simply factored out in the corresponding time-dependent Schrödinger equation for the electron.

When considering ionization cross sections integrated over the momentum transfer (i.e. electron emission spectra) the effect of the $p-n$ interaction can be roughly estimated in our case as proportional to m_e/M_p. Thus, this interaction plays practically no role in forming electron emission spectra.

Energy spectrum

Energy spectra of electrons ejected from the hydrogen ground state in collisions with protons and antiprotons are displayed in figure 9. For collisions at $v_p = 3$ there is a noticeable difference between CDW-EIS results for protons and antiprotons. This also implies that the CDW-EIS results considerably differ from first Born predictions. In figure 9 it is clearly observed that, according to the CDW-EIS theory, protons are more effective in producing emission from the hydrogen ground state, except for very low-energy electrons where collisions with both projectiles yield identical spectra. The relative "productivity" of protons compared to antiprotons increases with increasing emission energy reaching approximately a factor of $1.2-1.25$ for an electron energy $E = 1$ a.u..

As expected, when the collision velocity increases, the differences in the electron energy distributions due to proton and antiproton impact decrease and the CDW-EIS results tend to converge with first Born predictions.

Longitudinal momentum distribution

Electron emission cross sections differential in the longitudinal component $k_{||}$ of the total electron momentum $\mathbf{k}$ are shown in Figure 10. These cross sections were obtained by taking into account only those emitted electrons which have the "transverse kinetic energy" $k_{\perp}^2/2 \leq 1$ a.u.. The longitudinal momentum spectra at the collision velocities $v_p = 3$ and 6 a.u. show a remarkable asymmetry in the electron emission: a majority of the emitted electrons has a positive longitudinal velocity component, i.e. $\mathbf{k} \cdot \mathbf{v}_p > 0$. Such an asymmetry is known for collisions with highly charged ions where it is often attributed solely to the post-collision interaction between the projectile and the emitted electron [26]. However, according to figure 10, even the first Born theory, which completely ignores the post-collision interaction, suggests a strong asymmetry in the electron emission with a main part of ejected electrons moving in the direction of the projectile velocity. Moreover, CDW-EIS calculations, which include the post-collision effect [25], suggest that even for collisions with antiprotons, where the Coulomb field of the outgoing projectile pushes the electron backwards, the electrons still tend to be emitted mainly in the forward direction although the relative number of these electrons, according to the CDW-EIS theory, is substantially smaller than in collisions with protons. As was noted in [27] the longitudinal asymmetry in the electron emission in fast enough collisions can be qualitatively understood as arising due to the interplay of the following two main factors. One is the post-collision interaction, in which an outgoing projectile, by attracting or repelling an emitted electron, tries to push it in the forward or backward directions, respectively. The second, which is usually more important unless the projectile charge reaches relatively high values, is connected with the minimum momentum transfer q_{min} which can be interpreted as the longitudinal component of the momentum of a virtual photon representing the moving projectile field. Once the photon is absorbed, its momentum is transferred to the target leading to the recoil of the target. For $q_{min} > 0$, as is the case for ionization, the latter recoil always pushes the emitted electron in the forward direction independently of the sign of the projectile charge.

Transverse momentum distribution

Transverse momentum distributions of the emitted electrons are presented in figure 11. These distributions were obtained by integrating over the longitudinal momentum component of the emitted electrons from -1 a.u. to 1 a.u.. It is seen that in the electron transverse momentum plane the difference between CDW-EIS results for hydrogen ionization by protons and antiprotons is not so large as that for the longitudinal electron spectra. This can be attributed to the fact that the post-collision interaction is less effective in influencing electron motion in the plane perpendicular to the projectile velocity.

Only for the lowest considered velocity, $v_p = 3$ a.u., one observes that there is a substantial difference between the electron transverse momentum distributions due to proton and antiproton impact. If one restricts attention to ejected electrons with $-1 \leq k_{\|} \leq 1$ then, according to CDW-EIS calculations, protons are more effective in producing electrons with lower values of $k_\perp$ ($k_\perp < 0.83 - 0.89$) whereas collisions with antiprotons produce more electrons with $k_\perp > 0.83 - 0.89$. The latter of course does not contradict the finding that, in equivelocity collisions, protons produce more soft electrons at each electron emission energy [28]. It simply suggests that antiprotons can be more effective in making that part of hydrogen ionization where the emitted electrons have some specific relations between $k_\perp$ and $k_{\|}$.

Summary

Using the first and second Born and CDW-EIS approximations we have considered hydrogen ionization with emission of soft electrons in collisions with equivelocity protons and antiprotons at $3 \leq v_p \leq 6$. One of the main conclusions of the present study is that there exist substantial charge-sign effects in the ionization dynamics. These effects are most pronounced in the fully differential emission pattern but they also "survive" even in the total ionization cross section suggesting, in particular, that protons are more effective, compared to antiprotons, in producing soft electron emission in the range of impact velocities under consideration.

We have discussed in some detail the role of i) the interaction between the projectile and the target nucleus and of ii) multiple photon exchanges between the projectile and the target

electron. According to the first Born approximation both points i) and ii) should have no influence on hydrogen ionization.

It was found that the effect of the multiple interactions between the projectile and the target electron on the projectile scattering is more pronounced in collisions with relatively small Q and that it rapidly decreases when Q increases.

The $p-n$ interaction was found to represent an important mechanism of momentum exchange in the collisions. It has been shown that this mechanism has a substantial effect on the projectile scattering not only when the transverse momentum transfer Q approaches values corresponding to the "critical" scattering angle $\vartheta_{max} = m_e/M_p$ but also for smaller Q. Thus, in contrast to the multiple interactions between the projectile and the target electron, the $p-n$ interaction considerably influences the projectile scattering in the whole range of Q considered in this paper.

However, the effect of the latter interaction on ionization cross sections integrated over the momentum transfer, turns out to be negligible. The reasons for this are the very large (compared to electron) masses of the projectile and the target nucleus that results in extremely small projectile deflection angles and very low recoil velocities of the target nucleus. Because of this the $p-n$ interaction does not lead to ionization and does not change the interaction between the projectile and the target electron. Thus, the $p-n$ interaction just "redistributes" the projectile scattering probabilities between different (very small) scattering angles.

In contrast, the multiple interactions between the projectile and the target electron may substantially influence ionization cross sections integrated over the momentum transfer. Although the most prominent effect of these interactions is the post-collision one, which is also mainly "redistributive" in its nature, they may affect even the total ionization cross section. In particular, they are responsible for the differences in the electron energy distributions and the total ionization cross sections in collisions with equivelocity protons and antiprotons.

We expect that the COLTRIMS techniques [29] will soon be extended to permit measurements of differential cross sections for ionization of atomic hydrogen. This will allow to test theoretical three-body Coulomb models for hydrogen ionization by heavy projectiles to

a very high level of accuracy and could boost further theoretical developments in this field.

---

[1] D.R.Schultz, Phys. Rev. **A 40** 2330 (1989)

[2] N.Toshima, Phys. Lett. **A 175** 2024 (1993)

[3] D.R.Schultz, P.S.Krstic, C.O.Reinhold, and J.C.Wells, Phys. Rev. Lett. **76** 2882 (1996)

[4] K.A.Hall, J.F.Reading and A.L.Ford, J.Phys. **B 29** 6123 (1996)

[5] X.-M.Tong, T.Watanabe, D.Kato, and S.Ohtani, Phys. Rev. **A 66** 032708 (2002)

[6] H.Knudsen, U.Mikkelsen, K.Paludan, K.Kirsebom, S.P.Møller, E.Uggerhøj, J.Slevin, M.Charlton, E.Morenzoni, Phys. Rev. Lett. **74** 4627 (1995)

[7] S.Jones and D.H.Madison, Phys. Rev. **A 65** 052727 (2002)

[8] M.Schulz, R.Moshammer, D.Fischer, H.Kollmus, D.Madison, S.Jones and J.Ullrich, Nature (in press)

[9] R.Moshammer, A.Perumal, M.Schulz, V.D.Rodriguez, H.Kolmus, R.Mann, S.Hagmann, and J.Ullrich, Phys. Rev. Lett. **87** 223201 (2001)

[10] M.Schulz, R.Moshammer, A.Perumal and J.Ullrich, J.Phys. **B 35** L161 (2002)

[11] R.E.Olson and J.Fiol, J.Phys. **B 34** L625 (2001)

[12] H.R.J.Walters, Phys. Rep. **116** 1 (1984)

[13] D.S.F.Crothers and J.F.McCann, J.Phys. **B 16** 3229 (1983)

[14] P.D.Fainstein, V.H.Ponce and R.D.Rivarola, J.Phys. **B 24** 3091 (1991)

[15] V.D.Rodrigues, J.Phys. **B 29** 275 (1996)

[16] S.Jones and D.H.Madison, Phys. Rev. Lett. **81** 2886 (1998)

[17] S.Jones and D.H.Madison, Phys. Rev. **A 62** 042701 (2000)

[18] Note that very recently a generalization of the CDW-EIS, GCDW-EIS, was proposed in [19].

[19] D.S.F.Crothers, D.M.McSherry, S.F.C.O'Rourke, M.B.Shah, C.McGrath, and H.B.Gilbody, Phys.Rev.Lett., **88** 053201 (2002)

[20] The right-hand side of (2) is also integrated over the angle $\varphi_{\mathbf{Q}}$ of the momentum $\mathbf{Q}$ that gives a factor 2π.

[21] Within the first order theory the target can be also ionized solely by the (single) $p-n$ interaction provided the momentum transferred to the target nucleus is so huge (on the target scale) that the recoil velocity of the latter becomes of order of the typical electron velocity

~ 1 a.u. in the target initial state. Such a "knock-out" mechanism, however, is not considered here since it would result in negligible cross sections.

[22] Of course, whether Q is "small", "intermediate" or "large" depends on the value of E_k.

[23] At this point we note that the role of the $p-n$ interaction for the singly differential (in Q) cross section for helium ionization by high-velocity protons and deuterons in collisions with large Q was investigated experimentally and theoretically in [24] and [15].

[24] E.Y.Kamber, C.L.Cocke, S.Cheng, J.H.McGuire and S.L.Varghese, J.Phys. **B 21** L455 (1988); A. Salin, J.Phys. **B 22** 3901 (1989); R.E.Olson, J.Ullrich, R.Dörner and H.Schmidt-Böcking, Phys. Rev. **A 40** 2843 (1989), J.Phys. **B 22** 3901 (1989); F.G.Kristensen and E.Horsdal-Pedersen, J.Phys. **B 23** 4129 (1990); X.Fang and J.F.Reading, NIM **B 53** 453 (1991); H.Fukuda, I.Shimamura, L.Vegh and T.Watanabe, Phys. Rev. **A 44** 1565 (1991); A.Gensmantel, J.Ullrich, R.Dörner, R.E.Olson, K.Ullmann, E.Forberich, S.Lencinas, and H.Schmidt-Böcking, Phys. Rev. **A 45** 4572 (1992); W.R.DeHaven, C.Dilley, A.Landers, E.Y.Kamber, and C.L.Cocke, Phys. Rev. **A 57** 292 (1998)

[25] Due to the presence of the eikonal phase in the initial state the CDW-EIS approach also includes the "pre-collision" effect. In this paper the term "post-collision" denotes the total effect of both post- and pre- collision interactions.

[26] R.Moshammer et al, Phys. Rev. Lett. **73** 3371 (1994)

[27] A.B.Voitkiv, J.Phys. **B 29** 5433 (1996); A.B.Voitkiv, N.Grün and W.Scheid, J.Phys. **B 32** 3923 (1999)

[28] This has been checked for $E_k \leq 4$ a.u..

[29] R.Dörner, V. Mergel, O. Jagutzki, L. Spielberger, J. Ullrich, R. Moshammer and H. Schmidt-Böcking, Phys. Rep. **330** NN2-3 95 (2000)

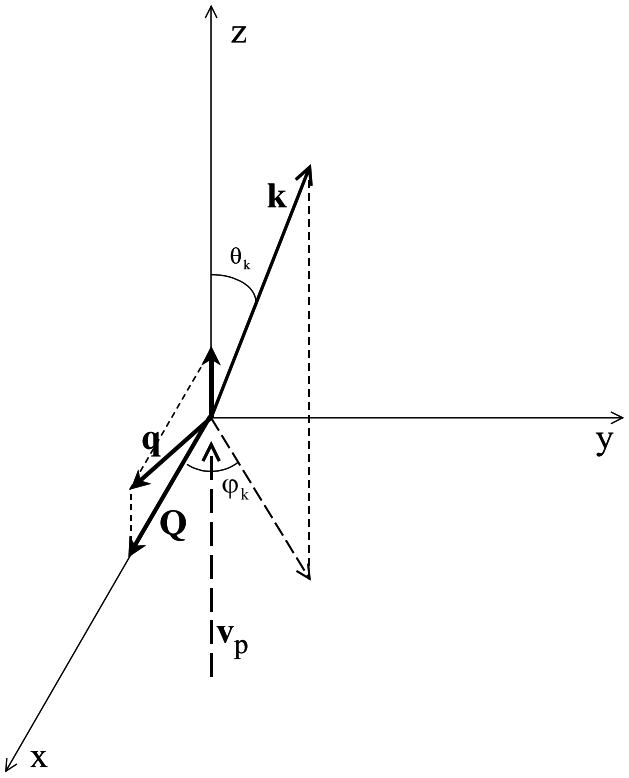

Figure 1

FIG. 1: The collision geometry.

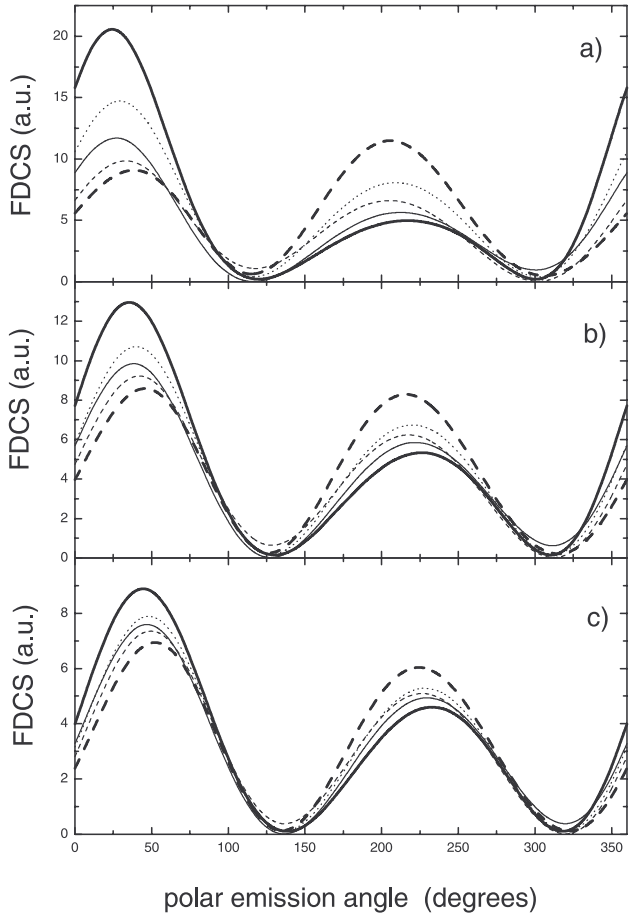

Figure 2

FIG. 2: Fully differential cross section (FDCS) in the collision plane. The collision parameters: $v_p = 3$ (a), 4.5 (b) and 6 (c), respectively; $E_k = 1$ eV, $Q = 0.1$ a.u. and $\varphi_k = 0^0$. Thick solid curve: CDW-EIS results for a proton impact, the $p - n$ interaction is included. Thin solid curve: CDW-EIS results for a proton impact, the $p-n$ interaction is ignored. Thick dash curve: CDW-EIS results for an antiproton impact, the $p - n$ interaction is included. Thin dash curve: CDW-EIS results for an antiproton impact, the $p - n$ interaction is ignored. Dot curve: first Born results.

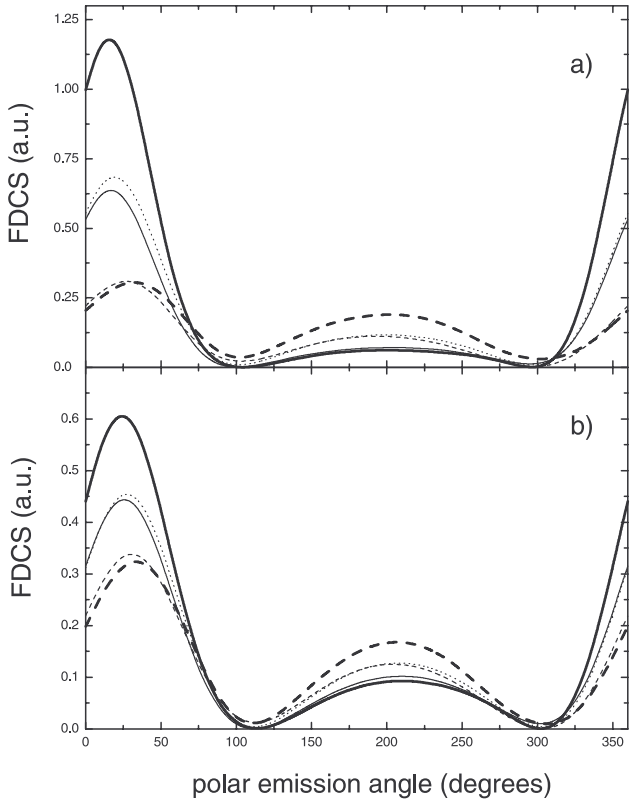

Figure 3

FIG. 3: FDCS in the collision plane. The collision parameters: $v_p = 3$ (a)and 4.5 (b), respectively; $E_k = 10$ eV, $Q = 0.1$ a.u. and $\varphi_k = 0^0$. Results of the CDW-EIS and first Born approximations are labelled by the same types of curves as in figure 2.

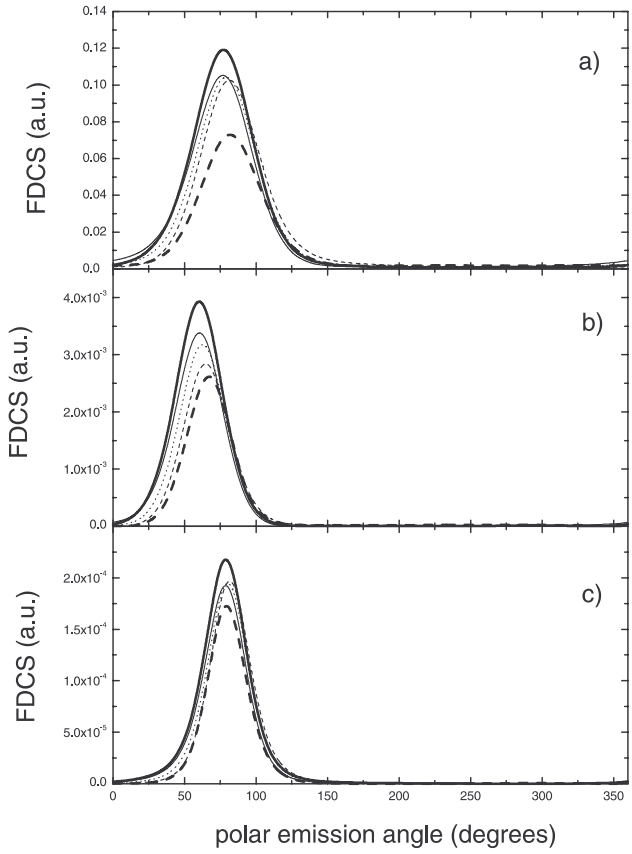

Figure 4

FIG. 4: FDCS in the collision plane. The collision parameters: $v_p = 3$ (a)and 4.5 (b), respectively; $E_k = 10$ eV, $Q = 0.1$ a.u. and $\varphi_k = 0^0$. Results of the CDW-EIS and first Born approximations are labelled by the same types of curves as in figure 2.

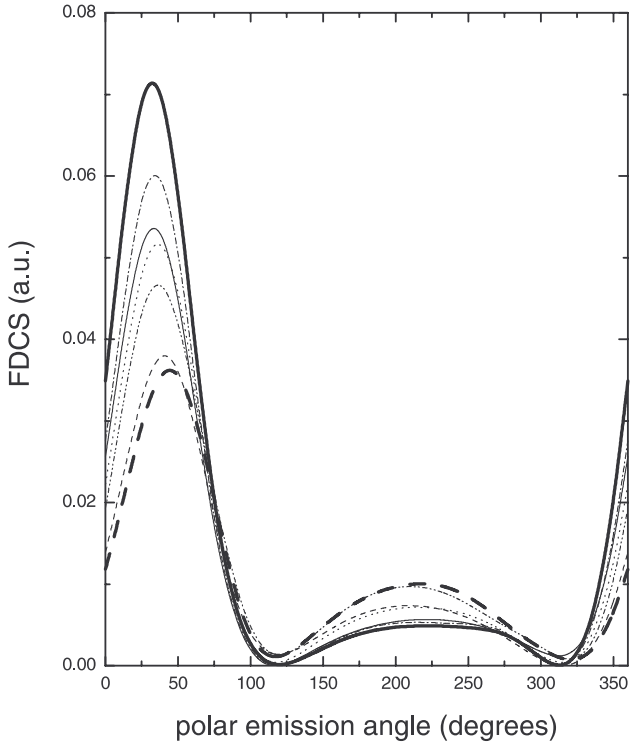

Figure 5

FIG. 5: FDCS in the collision plane. The collision parameters: $v_p = 4.5$, $E_k = 20$ eV, $Q = 0.2$ a.u.. Results of the CDW-EIS and first Born approximations are labelled by the same types of curves as in figure 2. In addition, thin dash-dot and dash-dot-dot curves represent second Born results for protons and antiprotons, respectively.

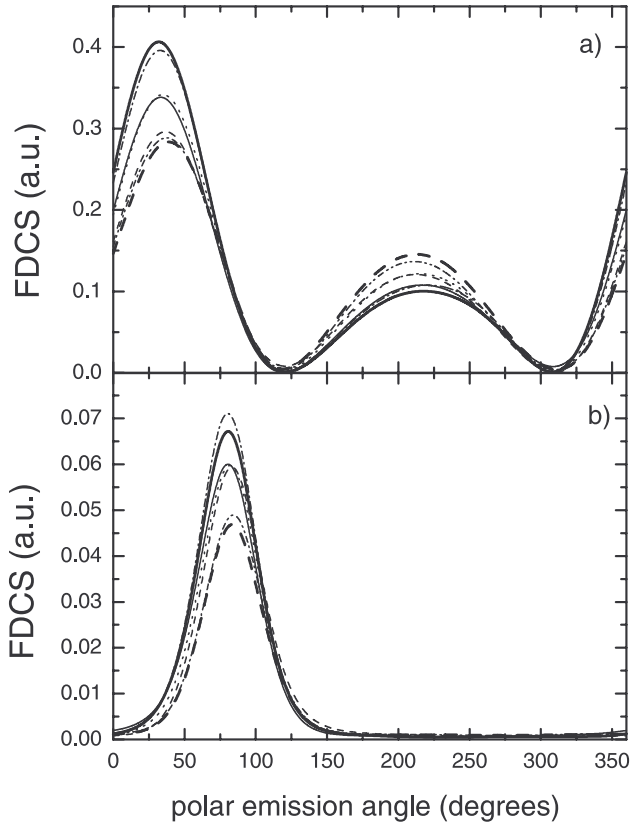

Figure 6

FIG. 6: FDCS in the collision plane. The collision parameters: $v_p = 4.5$, $E_k = 20$ eV, $Q = 0.2$ a.u.. Results of the CDW-EIS and first Born approximations are labelled by the same types of curves as in figure 2. In addition, thin dash-dot and dash-dot-dot curves represent second Born results for protons and antiprotons, respectively.

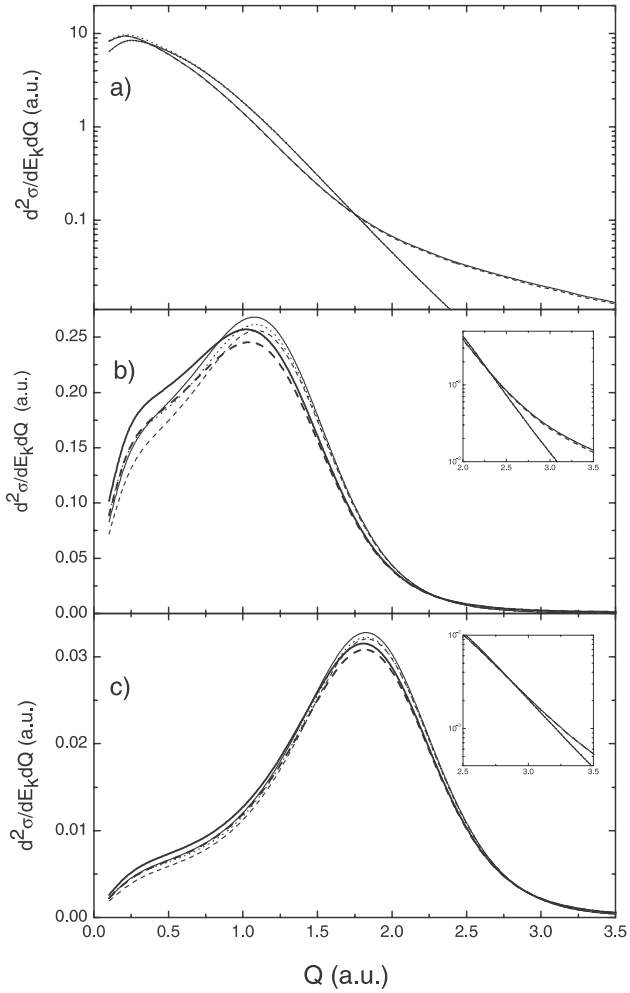

Figure 7

FIG. 7: $d^2\sigma/dQdE_k$ as a function of Q for: a) $v_p = 3$ a.u. and $E_k = 1$ eV; b) $v_p = 4.5$ a.u. and $E_k = 20$ eV, in order to see the differences between the cross sections at the larger Q the range $2 \leq Q \leq 3.5$ is also shown in the inset; c) $v_p = 6$ a.u. and $E_k = 50$ eV, in order to see the differences between the cross sections at the larger Q the range $2.5 \leq Q \leq 3.5$ is also shown in the inset. Results of the CDW-EIS and first Born approximations are labelled by the same types of curves as in figure 2.

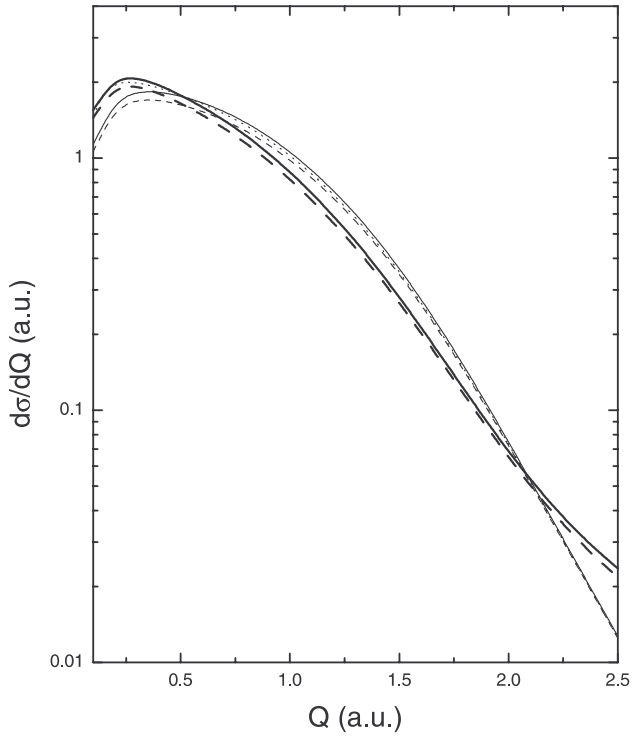

Figure 8

FIG. 8: Cross section $d\sigma/dQ$ obtained by the integration over all emitted electrons with energies $E_k \leq 1$ a.u.. The collision velocity $v_p = 3$ a.u.. Results of the CDW-EIS and first Born approximations are labelled by the same types of curves as in figure 2.

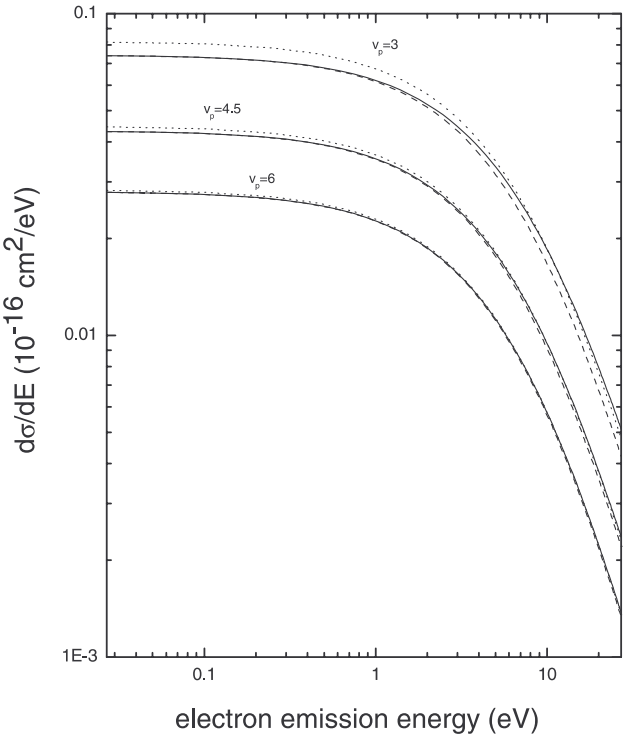

Figure 9

FIG. 9: Energy spectra of emitted electrons. Collision velocity: $v_p = 3$, 4.5 and 6 a.u. (denoted in the figure). Dot curve: first Born results. Solid curve: CDW-EIS results for proton impact. Dash curve: CDW-EIS results for antiproton impact.

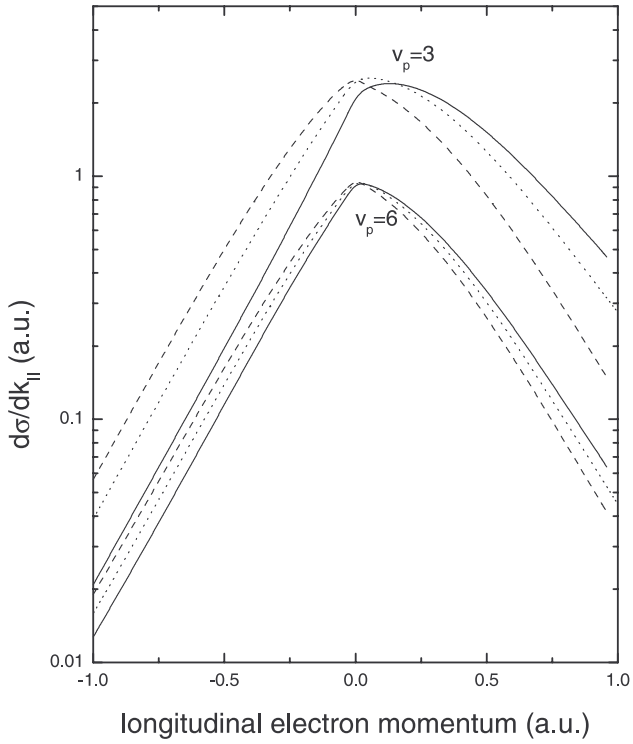

Figure 10

FIG. 10: Longitudinal momentum spectra of emitted electrons. Collision velocity: $v_p = 3$ and 6 a.u. (denoted in the figure). Dot curve: first Born results. Solid curve: CDW-EIS results for proton impact. Dash curve: CDW-EIS results for antiproton impact.

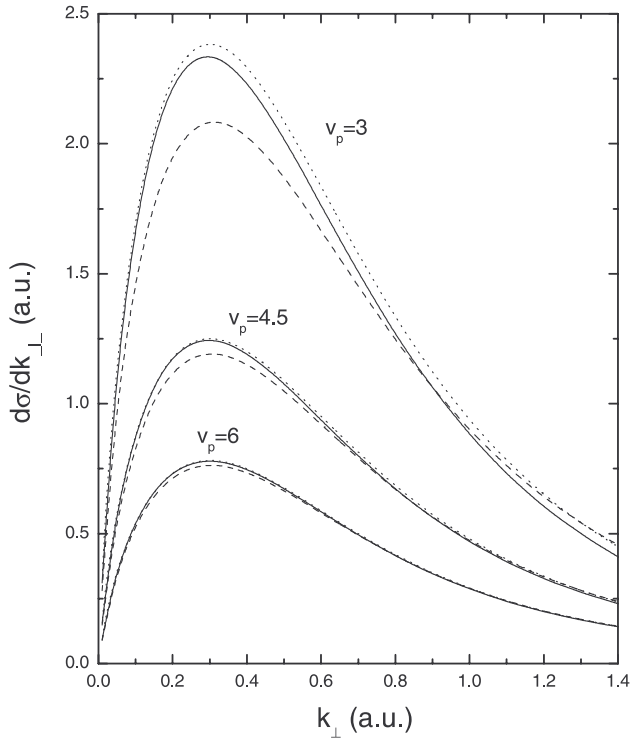

Figure 11

FIG. 11: Transverse momentum spectra of emitted electrons. Collision velocity: $v_p = 3$, 4.5 and 6 a.u. (denoted in the figure). Dot curve: first Born results. Solid curve: CDW-EIS results for proton impact. Dash curve: CDW-EIS results for antiproton impact.